Channel Estimation for Ultra-Wideband Communications

Vincenzo Lottici, Aldo D'Andrea, *Senior Member, IEEE*, and Umberto Mengali, *Life Fellow, IEEE*

***Abstract*—This paper deals with channel estimation in ultra-wideband communications operating in a multipath environment and in the presence of multiaccess interference. The channel parameters are the attenuations and delays incurred by the signal echoes along the propagation paths. Time-hopping modulation with binary symbols is assumed. The estimation method is based on the maximum-likelihoodcriterion and is applied to two different scenarios: either with known symbols (DA estimation) or with unknown symbols (NDA estimation). The effects of the estimation errors on the performance of a Rake receiver are assessed by simulation by comparing the receiver bit-error rate with either perfect channel estimates or imperfect estimates as obtained from the proposed algorithms. The results show that the degradations are tolerable as long as the number of users is limited. They also show that the DA method has an edge over the NDA in that it can handle a larger number of users for a fixed degradation. The number of users that can be accommodated in practice is found for some values of the system parameters.**

***Index Terms*—Channel estimation, synchronization, ultra-wideband (UWB) communications.**

I. Introduction

RECENT work in the area of wireless systems indicates that ultra-wideband (UWB) radio is a viable technology for short-range multiple-access communications. The interested reader is referred to [1]–[4] for an overview on this signaling format and in depth discussions on its potential to countering multiple-access interference (MAI) and multipath propagation.

UWB techniques have several attractive qualities. As they involve trains of very short pulses (typically on the order of a nanosecond), it is possible to resolve and combine signal echoes with path length differentials down to about 30 cm, thereby exploiting the diversity inherent in the multipath channel. Second, as each pulse train is time-hopping and has a very low duty cycle, it suffers little interference from other pulse trains operating in the same environment. Third, the signal power is spread over a bandwidth so large that the transmitted spectral density has little impact on narrowband radio systems operating in frequency overlay. Finally, pulse trains are baseband signals (they are not modulated onto a carrier) and operate in the lowest possible frequency band. Therefore, they have the best chance of penetrating obstacles (walls, for example) that would be opaque at higher frequencies.

Manuscript received November 15, 2001; revised June 28, 2002. This work was supported in part by Marconi Mobile, Italy, under Grant 213/2002. This paper was presented at the 3rd International Workshop on Multicarrier Spread-Spectrum (MCSS 2001), Oberpfaffenhofen, Germany, September 26–28, 2001.

The authors are with the Department of Information Engineering, 56126 Pisa, Italy (e-mail: umberto.mengali@iet.unipi.it).

Digital Object Identifier 10.1109/JSAC.2002.805053

The following key issues must be addressed in the design of UWB systems. Consider first a single-path channel. As time-hopping is performed with code sequences that repeat periodically, a correlation receiver must know the beginning of each code cycle to successfully perform data detection. This is the usual timing acquisition problem commonly encountered in direct-sequence code-division multiple-access (DS-CDMA) applications. However, the problem here is exacerbated by the use of extremely narrow pulses. Timing errors in excess of a small fraction of nanosecond may cause dramatic performance losses.

In a multipath environment, the exploitation of the channel diversity calls for sophisticated receivers. Multiuser detection [5] is known to be the optimal solution but, as its complexity increases exponentially with the number of users, it is often impractical. Suboptimal schemes are indispensable. In this context the Rake receiver [6] is a good tradeoff between high-performance and low-complexity. In addition, it represents the building block for other schemes performing multiuser interference cancellation.

In a Rake receiver, each signal echo is correlated with a locally generated time-hopping pulse train and then combined into a single test variable for final decision. Time alignment is required between the code sequence in each echo and the corresponding locally generated reference. Also, the attenuations incurred by the various echoes must be known to maximize the signal-to-noise ratio (SNR) in the decision variable (maximal ratio combining). In conclusion, proper Rake operation requires information about the delays and attenuations of the channel paths. These parameters are collectively referred to as *channel parameters*.

The purpose of the present paper is to derive channel parameter estimates from the received waveform. In doing so we adopt a maximum-likelihood (ML) approach and consider two scenarios: either data-aided (DA) or nondata-aided (NDA) estimation. The first instance is of interest during channel *acquisition*, when a training sequence is available. Channel *tracking* can be pursued in a pilot-aided fashion, by periodically retransmitting the training sequence, or in a decision-directed (DD) manner using the receiver decisions in place of the true data. On the other hand, NDA estimation is useful in broadcast networks where training sequences would impede the transmitter when new users enter the network.

Channel parameter estimation in UWB communications has been previously addressed in [7] to assess the signal energy capture in Rake receivers as a function of the number of the Rake fingers. Basically, an isolated monocycle is transmitted through the channel and the corresponding received waveform is recorded. The problem is to approximate the actual channel

with a channel with L_c branches and to choose the propagation parameters in the latter in such a way that its output matches the recorded waveform as best as possible. Clearly, the degree of matching depends on L_c and the minimum value of L_c required for a good match establishes the number of fingers that a Rake receiver must possess to efficiently exploit the channel diversity. The present paper is still concerned with channel estimation but our assumptions and purposes are different. Indeed, we derive channel estimates from the information-bearing signal rather than from isolated pulses and, secondly, we focus on the effects of estimation errors on the receiver performance.

The parameter estimation problem also arises in the context of DS-CDMA systems and the interested reader is referred to [8]–[10] for a representative sample of the results obtained in this area. Although the methods developed for DS-CDMA can be adapted to UWB systems, the much higher sampling rates in the latter call for different solutions.

The rest of the paper is organized as follows. In Section II, we discuss the signal model and recall the Rake's structure. DA estimation is investigated in Section II and NDA estimation in Section III. The performance of DA and NDA algorithms is assessed in Section IV by simulation. Finally, some conclusions are offered in Section VI.

II. Signal Format and Rake Receiver

The signal transmitted by the desired user is modeled as [1], [2]

$$s(t) = \sum_i b\left(t - iNT_f - a_i\Delta\right) \tag{1}$$

where

$$b(t) = \sum_{j=0}^{N-1} g(t - jT_f - c_jT_c). \tag{2}$$

In the last equation, $g(t)$ is the basic pulse used to convey information (referred to as *monocycle*) and T_f is the frame time, i.e., the separation between adjacent monocycles when the symbols c_j are identically zero. The ratio of T_f to the duration of the monocycle D_g is the *duty cycle* and may be on the order of a hundred or more. The sequence $\{c_i\}$ is the user's time-hopping code and its elements are integers taking values in the range $0 \leq c_j \leq N_h - 1$. The parameter T_c is the duration of an addressable time bin. In conclusion, the right hand side of (2) consists of a *block* of N time-hopped monocycles.

Equation (1) says that, if the a_i were all zero, the signal would be a repetition of $b(t)$-shaped blocks with period NT_f. However, the a_i are not identically zero. Indeed, they represent the data symbols and are modeled as binary (0 or 1) independent and identically distributed (i.i.d.) random variables. Correspondingly, Δ may be viewed as the time shift impressed by a unit data symbol on the monocycles of a block. It is intuitively clear that the choice of Δ affects the detection process and can be exploited to optimize system performance [1], [2]. To summarize, the transmitted signal consists of a sequence of $b(t)$-shaped position-modulated blocks.

Two remarks about this signal model are in order. From (1) and (2) it appears that the code sequence restarts at every data symbol. This "short-code" assumption is made here for the sake of simplicity and is in keeping with some trends in the design of third-generation CDMA cellular systems. Longer codes are conceivable and perhaps more attractive but lead to more complex channel estimation schemes. The second remark is about the distance between adjacent blocks in (1). It is easily seen that they may be partially overlapped, depending on the values of T_f, Δ, T_c and $\{c_i\}$. Overlapping is not desirable, however, as it generates intersymbol interference (ISI) and complicates the detection process. The minimum distance between the last monocycle in a block and the first in the next block is found to be $d_{\min} = T_f - \Delta - T_c(c_{N-1} - c_0)$. In the following, we assume that $d_{\min}$ is greater than *twice* the monocycle duration D_g. This guarantees that no ISI occurs at the output of a filter matched to $b(t)$ and, in consequence, optimum data detection can be performed in a symbol-by-symbol fashion.

When several time-hopping signals are simultaneously transmitted over a channel with L_c paths, the composite waveform at the output of the receiver antenna may be written as

$$r(t) = \sum_{l=1}^{L_c} \gamma_l s(t - \tau_l) + w(t) + m(t). \tag{3}$$

In this equation, $s(t)$ is the desired user's signal, γ_l and τ_l are the attenuation, and the delay affecting its replica traveling through the lth path, $w(t)$ is thermal noise and $m(t)$ represents the MAI caused by the other users. In writing (3), we have implicitly assumed a static channel, meaning that γ_l and τ_l are either fixed or vary so slowly that they are practically constant over several data symbols.

The optimum detection strategy for this multiple-access system leads to a multiuser receiver [5] which, however, is too complex to implement. More feasible schemes are of interest. The simplest suboptimal receiver is obtained making two approximations. First, the MAI is thought of as a white Gaussian process [1] and, as such, it can be lumped into the thermal noise in (3). The Gaussian approximation is justified by the central limit theorem if the users are many and have comparable powers. Second, a dominant path exists that conveys the major part of the desired user's energy. Under these assumptions (3) becomes

$$r(t) = \gamma_1 s(t - \tau_1) + w_{tot}(t) \tag{4}$$

where γ_1 is the largest path gain and $w_{tot}(t) = w(t) + m(t)$ is still a Gaussian and white process. Correspondingly, the minimum error probability is achieved by computing the correlation

$$y_k^{(1)} = \int_{kNT_f}^{(k+1)NT_f} r(t)v(t - kNT_f - \tau_1)\,dt \tag{5}$$

with $v(t) = b(t) - b(t - \Delta)$ and deciding that a_k equals either zero or one according to whether $y_k^{(1)}$ is greater or less than zero [1], [2]. As is clear from (2), the template signal $v(t)$ depends not only on the user's time-hopping code, but also on $g(t)$. For purposes of analysis, we assume that the shape of the monocycle is known [1].

The above detector may be viewed as a Rake receiver with a single finger (Rake-1). Note that, although Rake-1 needs to know the strongest path and the associated delay, it does not care

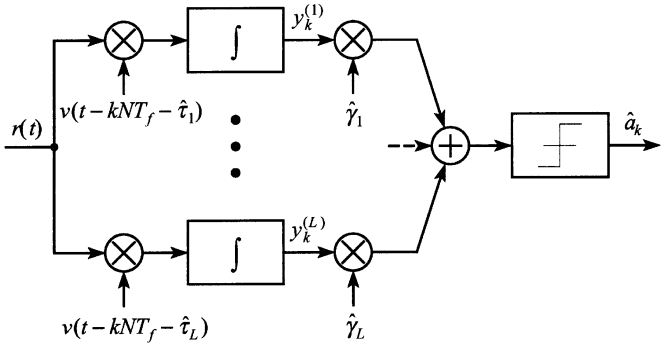

Fig. 1. Block diagram of a Rake-L receiver.

about the actual value of the path gain. A more efficient result is obtained by exploiting L signal echoes rather than just one. This leads to a Rake receiver with L fingers (Rake-L), whose block diagram is depicted in Fig. 1. The decision statistic is now the *maximal-ratio* combination of the correlators' outputs [6]

$$z_k = \sum_{l=1}^{L} \gamma_l \int_{kNT_f}^{(k+1)NT_f} r(t)v(t - kNT_f - \tau_l)\,dt. \quad (6)$$

In practice, the parameters $\{\gamma_l\}$ and $\{\tau_l\}$ are not known *a priori* and must be estimated. This is just the problem we address in the remainder of the paper.

III. Data-Aided Estimation

In this section, we concentrate on channel parameter estimation when the data symbols are known. For heuristic reasons we adopt the model in (3) wherein $w(t) + m(t) = w_{tot}(t)$ is white and Gaussian. This amounts to ignoring the structure of the MAI and underestimating its effects [5]. Such effects however will be assessed later by simulation.

The setting is as follows. The received waveform is observed over an interval $0 \le t \le T_0$, with T_0 a multiple M of the symbol period NT_f. The overall noise $w_{tot}(t)$ has a spectral density $N_0/2$. The parameters $\boldsymbol{\gamma} = (\gamma_1, \gamma_2 \cdots \gamma_{L_c})$ and $\boldsymbol{\tau} = (\tau_1, \tau_2 \cdots \tau_{L_c})$ are viewed as unknown deterministic quantities and, for the time being, the number of paths L_c is taken as a known quantity. We use a notation of the type $\tilde{x}$ to indicate a trial value of a variable x and we define as

$$\tilde{s}(t) = \sum_{l=1}^{L_c} \tilde{\gamma}_l s(t - \tilde{\tau}_l) \quad (7)$$

a possible realization of the signal component in (4) corresponding to the channel parameters $\tilde{\boldsymbol{\gamma}}$ and $\tilde{\boldsymbol{\tau}}$. Then, the log-likelihood function of the pair $(\boldsymbol{\gamma}, \boldsymbol{\tau})$ takes the form [11]

$$\log[\Lambda(\tilde{\boldsymbol{\gamma}}, \tilde{\boldsymbol{\tau}})] = 2\int_0^{T_0} r(t)\tilde{s}(t)\,dt - \int_0^{T_0} \tilde{s}^2(t)\,dt. \quad (8)$$

A more convenient expression for $\log[\Lambda(\tilde{\boldsymbol{\gamma}}, \tilde{\boldsymbol{\tau}})]$ is obtained substituting (7) into (8) and neglecting the correlation between signal echoes, i.e., assuming

$$\frac{\int_0^{T_0} s(t - \tilde{\tau}_{l_1})s(t - \tilde{\tau}_{l_2})\,dt}{\int_0^{T_0} s^2(t)\,dt} \approx 0 \qquad l_1 \ne l_2. \quad (9)$$

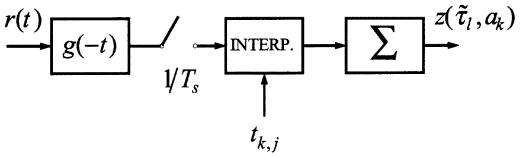

Fig. 2. Computation of sufficient statistics.

This approximation reflects the fact that, as the monocycles appearing in $s(t)$ are widely separated from each other, even a small time misalignment makes the echoes virtually orthogonal. Then, performing some ordinary manipulations, we get

$$\log[\Lambda(\tilde{\boldsymbol{\gamma}}, \tilde{\boldsymbol{\tau}})] = 2\sum_{l=1}^{L_c} \tilde{\gamma}_l \sum_{k=0}^{M-1} z_k(\tilde{\tau}_l, a_k) - ME_b \sum_{l=1}^{L_c} \tilde{\gamma}_l^2 \quad (10)$$

where E_b is the energy of $b(t)$

$$E_b = \int_0^{NT_f} b^2(t)\,dt \quad (11)$$

and $z_k(\tilde{\tau}_l, a_k)$ is response of the matched filter $b(-t)$ at $t = kNT_f + \Delta a_k + \tilde{\tau}_l$. Formally

$$z_k(\tilde{\tau}_l, a_k) = [r(t) \otimes b(-t)]_{t = kNT_f + \Delta a_k + \tilde{\tau}_l} \quad (12)$$

where $\otimes$ denotes convolution operation.

From (10) it is seen that $\{z_k(\tilde{\tau}_l, a_k)\}$ are sufficient statistics to compute the ML estimates of $(\boldsymbol{\gamma}, \boldsymbol{\tau})$. The calculation of these statistics can be carried out as follows. Inserting (2) into (12) yields

$$z_k(\tilde{\tau}_l, a_k) = \sum_{j=0}^{N-1} [r(t) \otimes g(-t)]_{t = (kN+j)T_f + \Delta a_k + \tilde{\tau}_l + c_j T_c} \quad (13)$$

which says that $z_k(\tilde{\tau}_l, a_k)$ is computed by feeding $r(t)$ to the filter matched to the monocycle and then sampling at the times $t_{k,j} = (kN + j)T_f + \Delta a_k + \tilde{\tau}_l + c_j T_c$, with $0 \le j \le N-1$. In practice the filter output is over-sampled at some suitable rate $1/T_s$ and the desired terms in the right-hand side of (13) are derived by interpolation as indicated in Fig. 2.

Returning to (10), our task is to maximize $\log[\Lambda(\tilde{\boldsymbol{\gamma}}, \tilde{\boldsymbol{\tau}})]$ as a function of $\tilde{\boldsymbol{\gamma}}$ and $\tilde{\boldsymbol{\tau}}$. This can be done in two steps. First, we vary $\tilde{\boldsymbol{\gamma}}$ while keeping $\tilde{\boldsymbol{\tau}}$ fixed. If the maximum is found at $\hat{\boldsymbol{\gamma}}(\tilde{\boldsymbol{\tau}})$, then (second step) we replace $\tilde{\boldsymbol{\gamma}}$ with $\hat{\boldsymbol{\gamma}}(\tilde{\boldsymbol{\tau}})$ in $\log[\Lambda(\tilde{\boldsymbol{\gamma}}, \tilde{\boldsymbol{\tau}})]$ and look for the maximum of $\log[\Lambda(\hat{\boldsymbol{\gamma}}(\tilde{\boldsymbol{\tau}}), \tilde{\boldsymbol{\tau}})]$.

The first step is straightforward and yields

$$\hat{\gamma}_l = \frac{1}{ME_b} J(\tilde{\tau}_l) \qquad 1 \le l \le L_c \quad (14)$$

with

$$J(\tilde{\tau}) = \sum_{k=0}^{M-1} z_k(\tilde{\tau}, a_k). \quad (15)$$

Next, substituting (14) into (10) it turns out that the problem reduces to maximizing

$$\sum_{l=1}^{L_c} J^2(\tilde{\tau}_l). \quad (16)$$

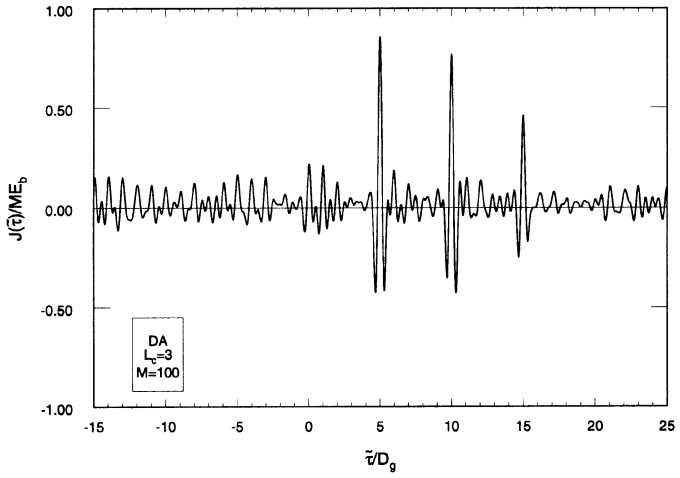

Fig. 3. Typical shape of $J(\tilde{\tau})/ME_b$.

As the maximum of (16) is found by maximizing each term in the sum, our problem reduces to looking for the locations of the *extrema* of $J(\tilde{\tau})$. Once they are found, the path gains follow from (14) recalling that γ_l is a positive quantity

$$\hat{\gamma}_l = \frac{1}{ME_b}\,|J(\hat{\tau}_l)| \qquad 1 \le l \le L_c. \tag{17}$$

Fig. 3 illustrates a typical shape of $J(\tilde{\tau})/ME_b$ as obtained with a three-path channel, ten users, and a SNR $E_b/N_0 = 10$ dB. An observation interval of a hundred symbols is chosen ($M = 100$) and the channel parameters are $\tau_l = l \times 5D_g$ ($l = 1, 2, 3$) and $\gamma_1 = 0.73$, $\gamma_2 = 0.67$, $\gamma_3 = 0.35$. It is seen that the three major positive peaks correspond to the signal echoes. However, the combined effect of noise and MAI also generates a number of other extrema (peaks). A first question is then: *which* peaks should we consider in a general situation? Stated in a different way, how can we distinguish signal echoes from artifacts of noise and MAI? From (17), we see that the largest peaks correspond to the strongest echoes. Thus, for high SNR values we expect that the L_c largest peaks are real echoes. On the other hand, since in practice we do not know the exact number of channel paths, *how many* peaks should we take? A reasonable answer is that, since in a Rake-L receiver we can only exploit L paths, we should limit ourselves to the L largest peaks. This strategy is adopted in the rest of the paper.

Some words are useful about the practical implementation of the DA method. A possible approach is to organize the data pattern in groups, each consisting of a preamble of M pilot symbols (*pilots* for short) followed by $Q \times M$ information symbols. The channel estimate from the pilots is used to detect the subsequent information data. In this context, the integer M must be large enough to guarantee adequate estimation accuracy. Simulations discussed later indicate that M must be on the order of a hundred or greater, depending on the estimation method (DA or NDA). Integer Q is related to the transmission efficiency $Q/(Q+1)$ and should be as large as possible. However, with a time-varying channel, the product $Q \times M$ must be much smaller than the channel decorrelation time (expressed in symbol intervals).

Another approach is to employ a DD technique. The symbol pattern has still a framed structure as before but the channel estimates are no longer "frozen" during the transmission of the data. Indeed, the detector decisions are taken in groups of M and are used in place of the true symbols to update the channel estimate. The advantage of this method is that it can track the channel and, in consequence, it allows using much larger values of Q. With a static channel we have found by simulation that the two methods have virtually the same performance at SNRs of practical interest. Therefore, in the following we report only on results obtained with the first method.

IV. Non Data-Aided Estimation

We investigate channel estimation when the symbols are unknown. In dealing with this problem, we still adopt a ML approach but, as we shall see, in the end we make a low SNR assumption to simplify the algorithm. The setting is as before, except that the symbols are now viewed as *nuisance* parameters, i.e., something we are not interested in. As indicated in [11], we can get rid of them by first computing the likelihood function for $\boldsymbol{a} = (a_0, a_1, \ldots, a_{M-1})$, $\boldsymbol{\gamma}$ and $\boldsymbol{\tau}$, say $\Lambda(\tilde{\boldsymbol{a}}, \tilde{\boldsymbol{\gamma}}, \tilde{\boldsymbol{\tau}})$, and then averaging over the probability density of $\tilde{\boldsymbol{a}}$. This produces the *marginal* likelihood function for $\boldsymbol{\gamma}, \boldsymbol{\tau}$

$$\Lambda(\tilde{\boldsymbol{\gamma}}, \tilde{\boldsymbol{\tau}}) = \int \Lambda(\tilde{\boldsymbol{\alpha}}, \tilde{\boldsymbol{\gamma}}, \tilde{\boldsymbol{\tau}}) p(\tilde{\boldsymbol{\alpha}})\, d\tilde{\boldsymbol{\alpha}} \tag{18}$$

from which the channel estimates are derived. As we have no specific knowledge of the data symbols, except that they are independent and take on values zero and one with the same probability, we model $p(\tilde{\boldsymbol{a}})$ as

$$p(\tilde{\boldsymbol{a}}) = \prod_{k=0}^{M-1} \frac{[\delta(\tilde{a}_k) + \delta(\tilde{a}_k - 1)]}{2} \tag{19}$$

where $\delta(\tilde{a})$ is the Dirac delta function.

Reasoning as in the previous section produces

$$\Lambda(\tilde{\boldsymbol{a}}, \tilde{\boldsymbol{\gamma}}, \tilde{\boldsymbol{\tau}}) = \exp\left\{\frac{1}{N_0}\left[2\sum_{l=1}^{L_c} \tilde{\gamma}_l \sum_{k=0}^{M-1} z_k(\tilde{\tau}_l, \tilde{a}_k) - ME_b \sum_{l=1}^{L_c} \tilde{\gamma}_l^2\right]\right\} \tag{20}$$

which can be rearranged as

$$\Lambda(\tilde{\boldsymbol{a}}, \tilde{\boldsymbol{\gamma}}, \tilde{\boldsymbol{\tau}}) = \exp\left\{\frac{-ME_b}{N_0} \sum_{l=1}^{L_c} \tilde{\gamma}_l^2\right\} \times \prod_{k=0}^{M-1} \exp\left\{\frac{2}{N_0} \sum_{l=1}^{L_c} \tilde{\gamma}_l z_k(\tilde{\tau}_l, \tilde{a}_k)\right\}. \tag{21}$$

Next, averaging as indicated in (18) provides the desired result

$$\Lambda(\tilde{\boldsymbol{\gamma}}, \tilde{\boldsymbol{\tau}}) = \exp\left\{\frac{-ME_b}{N_0} \sum_{l=1}^{L_c} \tilde{\gamma}_l^2\right\} \times \prod_{k=0}^{M-1} \left[\frac{1}{2}\exp\left\{\frac{2}{N_0} \sum_{l=1}^{L_c} \tilde{\gamma}_l z_k(\tilde{\tau}_l, 0)\right\} + \frac{1}{2}\exp\left\{\frac{2}{N_0} \sum_{l=1}^{L_c} \tilde{\gamma}_l z_k(\tilde{\tau}_l, 1)\right\}\right]. \tag{22}$$

The drawback with this expression is that the maximization is computationally intense since it requires a numerical search over the multidimensional space spanned by $(\tilde{\boldsymbol{\gamma}}, \tilde{\boldsymbol{\tau}})$. Moreover,

as the surface $\Lambda(\tilde{\boldsymbol{\gamma}}, \tilde{\boldsymbol{\tau}})$ might exhibit many spurious maxima, false locks would be possible with dramatic degradations in receiver performance. Some way out is needed to circumvent these obstacles.

As a first step in this direction we choose to maximize $\log(\Lambda(\tilde{\boldsymbol{\gamma}}, \tilde{\boldsymbol{\tau}}))$ rather than $\Lambda(\tilde{\boldsymbol{\gamma}}, \tilde{\boldsymbol{\tau}})$. From (22), we have

$$\log[\Lambda(\tilde{\boldsymbol{\gamma}}, \tilde{\boldsymbol{\tau}})] = \frac{-ME_b}{N_0} \sum_{l=1}^{L_c} \tilde{\gamma}_l^2 + \sum_{k=0}^{M-1} \times \log\left[\frac{1}{2}\exp\left\{\frac{2}{N_0}\sum_{l=1}^{L_c} \tilde{\gamma}_l z_k(\tilde{\tau}_l, 0)\right\} + \frac{1}{2}\exp\left\{\frac{2}{N_0}\sum_{l=1}^{L_c} \tilde{\gamma}_l z_k(\tilde{\tau}_l, 1)\right\}\right]. \quad (23)$$

Next we assume that the SNR is so low that the following approximation can be made in (23)

$$\log\left[\tfrac{1}{2}\exp\{2x\} + \tfrac{1}{2}\exp\{2y\}\right] \approx x + y \qquad |x|, |y| \ll 1. \quad (24)$$

Then, rearranging (23) yields

$$\log[\Lambda(\tilde{\boldsymbol{\gamma}}, \tilde{\boldsymbol{\tau}})] \approx 2\sum_{l=1}^{L_c} \tilde{\gamma}_l \sum_{k=0}^{M-1} \left[\frac{z_k(\tilde{\tau}_l, 0) + z_k(\tilde{\tau}_l, 1)}{2}\right] - ME_b \sum_{l=1}^{L_c} \tilde{\gamma}_l^2. \quad (25)$$

This result is rather interesting as it is quite similar to (10). In fact the two equations are identical, provided that $z_k(\tilde{\tau}_l, a_k)$ in (10) is replaced with $[z_k(\tilde{\tau}_l, 0) + z_k(\tilde{\tau}_l, 1)]/2$. It follows that the maximization method developed earlier is still valid with the indicated minor change.

A final comment on the heuristic character of (24) is worthwhile. The purpose of the approximation is to allow us to pass from (23) to (25), thereby dramatically simplifying the estimation algorithm. This does not necessarily imply that the actual SNR must be particularly low to guarantee that the estimation procedure based on (25) will work. Indeed, we shall see later that maximizing (25) still gives reasonable estimates even at ordinary values of SNR.

V. Performance Evaluation

The performance of the previous DA and NDA estimators has been assessed by simulation. With reference to (1) and (2) the following assumptions have been made. Following [12], we have chosen the monocycle shape as the second derivative of a Gaussian function (see Fig. 4)

$$g(t) = \left[1 - 16\pi\left(\frac{t - D_g/2}{D_g}\right)^2\right]\exp\left[-8\pi\left(\frac{t - D_g/2}{D_g}\right)^2\right]. \quad (26)$$

The monocycle duration D_g is taken as a time unit in the simulations. Time parameters in (1) and (2) are related to D_g by $\Delta = D_g$, $T_f = 40D_g$, and $T_c = T_f/20$. Note that a comparatively small duty cycle T_f/D_g of 40 is adopted to keep the simulation time within acceptable limits. Intuitively, increasing the duty cycle reduces the MAI (for a fixed number of users) and improves the system performance [13]. The length N_h of the time-hopping code is taken equal to 20 and the code symbols are randomly picked up in the interval $0 \le c_j \le 19$. Some preliminary tests have established the receiver sensitivity to the sampling rate (see Fig. 2) when a parabolic interpolation is used. The results shown later correspond to $T_s = 0.04D_g$ (25 samples per monocycle), but they are practically unchanged with $T_s = 0.08D_g$. Significant degradations take place as from $T_s = 0.16D_g$.

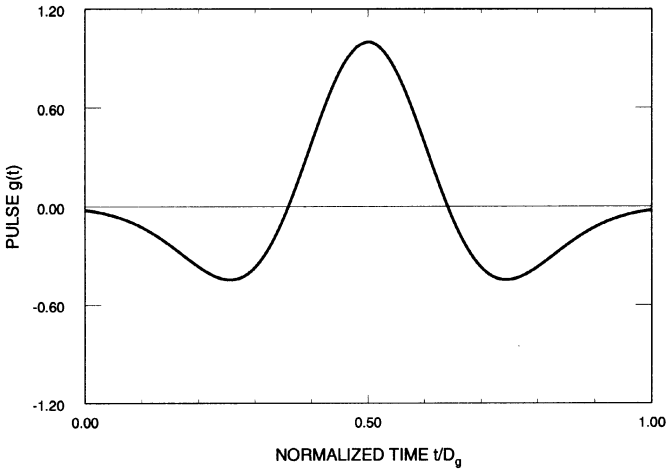

Fig. 4. Shape of the monocycle.

A total of N_u users are considered, each experiencing a channel with L_c paths. Again, to keep the simulation time within tolerable limits we have set $L_c \le 5$, even though L_c may be much higher in a dense multipath environment [7]. Path delays are fixed and equal to $\tau_l = 5lD_g$ $(l = 1, 2, \ldots L_c)$, the same for all the users. They are compatible with an office-building environment when D_g is on the order of a nanosecond. Path gains vary from user to user and are modeled as independent random variables with a Rayleigh distribution [14]. They have an exponential delay profile in which the expectations $E\{\gamma_l^2\}$ are proportional to $e^{-l/4}$ $(l = 1, 2, \ldots L_c)$. Most of the simulations assume that the users have the same average power (perfect power control). The individual signals contributing to MAI in (3) have the form indicated in (1), except that their time origins are randomized over $(0, NT_f)$ to reflect an asynchronous access to the channel.

An idea of the estimation accuracy of the DA and NDA algorithms is gathered from the following experiment in which three-path channels ($L_c = 3$) are assumed. The desired user's channel has fixed path gains ($\gamma_1 = 0.73, \gamma_2 = 0.67, \gamma_3 = 0.35$) while the other gains vary from run to run with the Rayleigh distribution mentioned above. Figs. 5 and 6 illustrate the standard deviation in the estimation of (τ_1, γ_1) with an observation length of 100 symbols $(M = 100)$. Timing errors are normalized to the monocycle duration while gain errors are normalized to 0.73. It is seen that the timing errors are on the order of a hundredth of the monocycle duration and (as expected) DA is superior to NDA. Also, with the only exception of the single-user curve in Fig. 5, all the other curves exhibit a floor ascribable to MAI. At first sight it is surprising that even the single-user curve

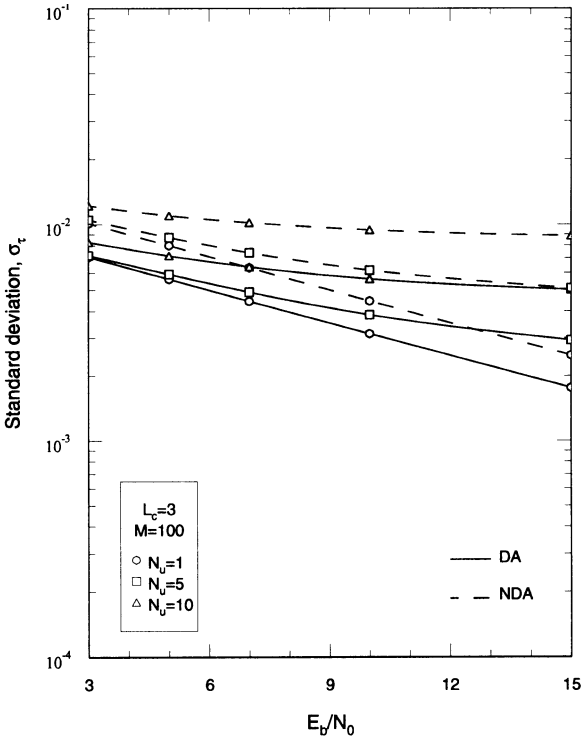

Fig. 5. Standard deviation of the delay estimates.

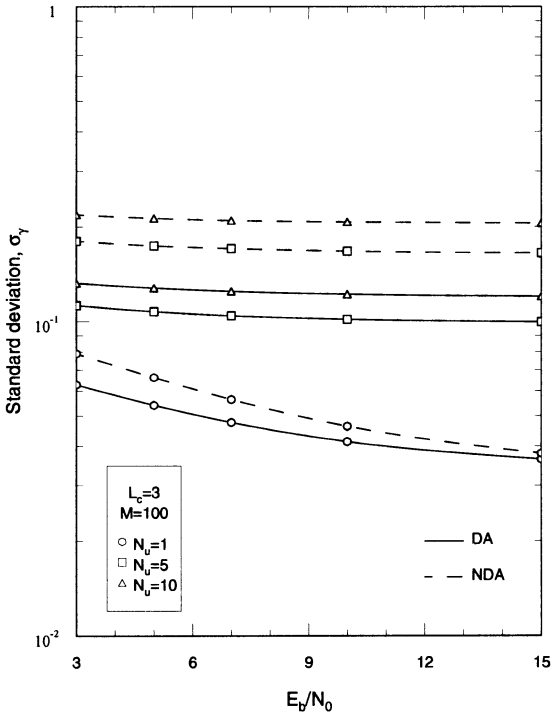

Fig. 6. Standard deviation of the gain estimates.

in Fig. 6 has a floor, since there is no MAI in this case. The explanation is that the floor is due to interpolation errors and, in fact, we have found that it disappears when the sampling rate is increased.

BER performance has been assessed with Rake-1 and Rake-3. The simulations are organized in cycles of a thousand symbols each. A cycle begins with the generation of the path gains for

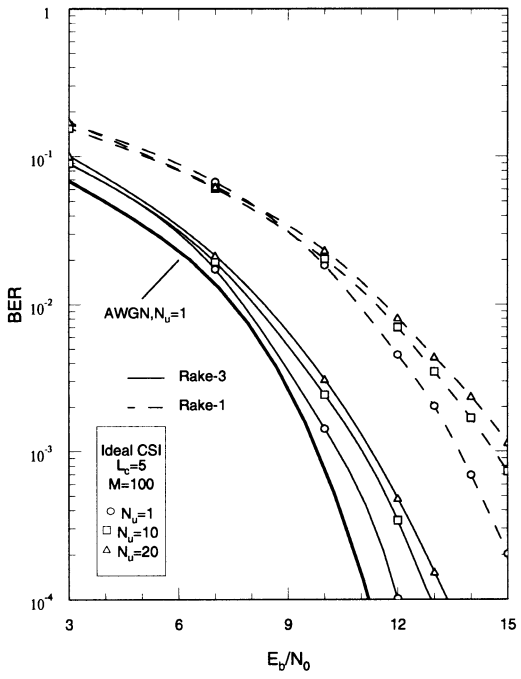

Fig. 7. BER curves with ideal CSI.

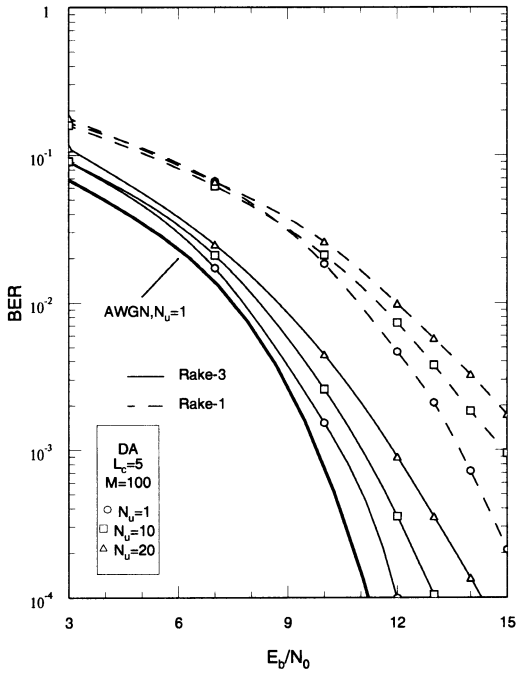

Fig. 8. BER curves with DA estimation.

all the users. Then, the channel parameters of the desired user are estimated over a window of a hundred symbols ($M = 100$) and are passed to the receiver's detector for use in the next 900 symbol intervals. The simulation stops when 200 decision errors are accumulated and the ratio of these errors to the total number of transmitted symbols is taken as an estimate of the BER.

Figs. 7–9 illustrate the BER performance in three cases: 1) ideal channel state information (CSI) (meaning that the desired user's parameters are perfectly known); 2) DA estimation; and 3) NDA estimation. Five-path channels are assumed ($L_c = 5$) and the number of users N_u ranges from 1 to 20. The

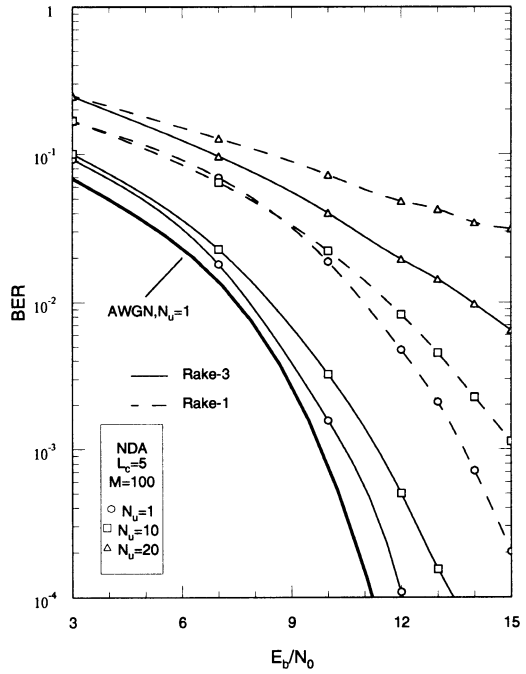

Fig. 9. BER curves with NDA estimation.

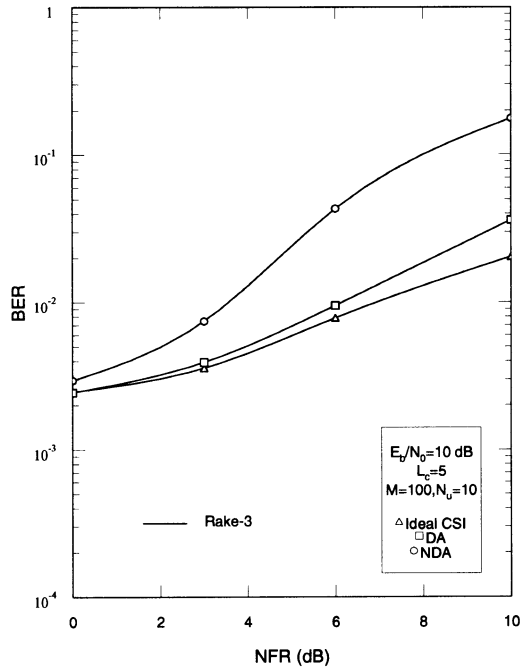

Fig. 10. BER performance versus NFR.

bottom line in each figure represents the receiver performance over a Gaussian channel with no MAI. Comparisons of Figs. 8 and 9 with Fig. 7 show the effects of channel estimation errors. Degradations with respect to ideal CSI depend on the number of Rake fingers, the estimation method, and the number of users. Rake-1 is simpler than Rake-3, but has poorer performance as it exploits a smaller fraction of the available signal energy. Also, DA is better than NDA (as expected). For example, with 20 users, Rake-3 with DA channel estimation has a BER degradation of only 1 dB (as compared with ideal CSI) in terms of SNR at BER $= 10^{-4}$. Vice versa, under the same operating conditions the loss incurred with NDA estimation is substantial. Things improve somewhat by increasing the observation window. For example, we have found that at $E_b/N_0 = 15$ dB the BER of Rake-3 decreases from 6×10^{-3} to 1.7×10^{-3} in passing from $M = 100$ to $M = 10.000$.

So far perfect power control has been assumed. Fig. 10 illustrates the impact of strong-powered interferers. Now all the users have the same power P_u, except for the desired user who has power P_d. The near–far ratio (NFR) is defined as P_u/P_d. The figure indicates that, with ten users and Rake-3, DA estimation is rather robust against strong interferers. In particular the receiver loses about 1 dB as compared with ideal CSI when NFR is as high as 10 dB. Vice versa with NDA estimation the receiver performance degrades rapidly as NFR increases.

VI. Conclusion

We have investigated channel parameter estimation for UWB systems operating in a multipath environment and in the presence of MAI. Two estimation schemes have been proposed, DA and NDA, both based on the ML criterion. In deriving these algorithms, we have approximated the MAI as white Gaussian noise, but the real effects of multiaccess interference have been assessed by simulation.

The influence of estimation errors on the operation of a Rake receiver has been evaluated by comparing the BER performance with either perfect channel estimates, or imperfect estimates obtained from the DA/NDA algorithms. A comparatively small duty cycle (of 40) has been adopted to keep the simulation time within acceptable limits. Also, perfect power control and an estimation window of 100 symbols have been generally assumed. In these conditions, we have found that up to 20 users can be accommodated with limited BER degradations provided that DA estimation is used. The NDA method is poorer and can accommodate only about ten users.

References

[1] M. Z. Win and R. A. Scholtz, "Ultra-wide bandwidth time-hopping spread-spectrum impulse radio for wireless multiple-access communications," *IEEE Trans. Commun.*, vol. 48, pp. 679–691, Apr. 2000.

[2] ——, "Impulse radio: How it works," *IEEE Commun. Lett.*, vol. 2, pp. 10–12, Jan. 1998.

[3] M. Z. Win, R. A. Scholtz, and M. A. Barnes, "Ultra-wide bandwidth signal propagation for indoor wireless communications," in *Proc. IEEE Int. Conf. Communication*, vol. 1, Montreal, Canada, June 1997, pp. 56–60.

[4] M. Z. Win and R. A. Scholtz, "On the robustness of ultra-wide bandwidth signals in dense multipath environments," *IEEE Commun. Lett.*, vol. 2, pp. 51–53, Feb. 1998.

[5] S. Verdù, *Multiuser Detection*. Cambridge , U.K.: Cambridge University Press, 1998.

[6] G. L. Turin, "Introduction to spread-spectrum antimultipath techniques and their application to urban digital radio," *Proc. IEEE*, vol. 68, pp. 328–353, Mar. 1980.

[7] M. Z. Win and R. A. Sholtz, "On the energy capture of ultrawide bandwidth signals in dense multipath environments," *IEEE Commun. Lett.*, vol. 2, pp. 245–247, Sept. 1998.

[8] S. E. Bensley and B. Aazhang, "Maximum likelihood synchronization of a single user code-division multiple-access communication systems," *IEEE Trans. Commun.*, vol. 46, pp. 392–399, Mar. 1998.

[9] E. G. Strom and F. Malmsten, "A maximum likelihood approach for estimating DS-CDMA multipath fading channels," *IEEE J. Select. Areas Commun.*, vol. 18, pp. 132–140, Jan. 2000.

[10] V. Tripathi, A. Mantravati, and V. V. Veeravalli, "Channel acquisition for wideband CDMA signals," *IEEE J. Select. Areas Commun.*, vol. 18, pp. 1483–1494, Aug. 2000.
[11] S. M. Kay, *Fundamentals of Statistical Signal Processing: Estimation Theory*. Englewood Cliffs: Prentice-Hall, 1993.
[12] F. Ramirez-Mireles, "Performance of ultra wideband SSMA using time-hopping and M-Ary PPM," *IEEE J. Select. Areas Commun.*, vol. 19, pp. 1186–1196, June 2001.
[13] L. Zhao and A. M. Haimovich, "Performance of ultra-wideband communications in the presence of interference," in *Proc. IEEE Int. Conf. Communications (ICC'01)*, Helsinki, Finland, June 2001, pp. 2948–2952.
[14] A. A. M. Saleh and R. A. Valenzuela, "A statistical model for indoor multipath propagation," *IEEE J. Select. Areas Commun.*, vol. 5, pp. 128–137, Feb. 1987.

Vincenzo Lottici received the Dr.Ing. degree (*cum laude*) in electronic engineering from the University of Pisa, Italy, in 1985.

From 1987 to 1992, he worked with several private companies in the design and development of digital signal processing systems. Since 1992, he has been with the Department of Information Engineering, University of Pisa, where he is currently a Research Fellow in Telecommunications. His research interests are in the field of analysis and simulation of digital transmission systems, and synchronization techniques.

Aldo N. D'Andrea (M'82–SM'91) received the Dr.Ing. degree in electronic engineering from the University of Pisa, Italy, in 1977.

From 1977 to 1981, he was a Research Fellow of the Italian National Research Council (CNR), at the Centro Studi per i Metodi e i Dispositivi di Radiotrasmissione (CSMDR), engaged in research on digital phase-lock loops and in the development of the Italian Air Traffic Control Program (ATC). From 1981 to 1987, he was a Research Scientist, Instituto di Elettronica e Telecommunicazioni, Universit of Pisa, where he is currently a Full Professor of Communication Systems. His interests include the design and analysis of digital communication systems, signal processing, and synchronization.

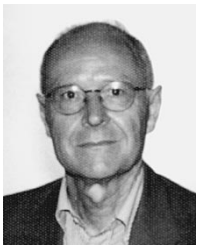

Umberto Mengali (M'69–SM'85–F'90–LF'03) received his education in electrical engineering from the University of Pisa, Italy. In 1971, he received the Libera Docenza degree in telecommunications from the Italian Education Ministry.

Since 1963, he has been with the Department of Information Engineering, University of Pisa, where he is a Professor of Telecommunications. In 1994, he was a Visiting Professor, University of Canterbury, New Zealand as an Erskine Fellow. His research interests are in digital communications and communication theory, with emphasis on synchronization methods and modulation techniques. He has published over 90 journal papers and has coauthored the book *Synchronization Techniques for Digital Receivers* (New York: Plenum Press, 1997). From 1997 to 2000, he has been an Editor of the *European Transactions on Telecommunications*.

Dr. Mengali is a Member of the Communication Theory Committee and has been an Editor of the IEEE TRANSACTIONS ON COMMUNICATIONS from 1986 to 1992.